ChemComm

Nitrogen-doped PtSn Nanocatalyst Supported on Hollow Silica Sphere for Acetic Acid Hydrogenation

Journal Name

Nitrogen-doped PtSn Nanocatalyst Supported on Hollow Silica Sphere for Acetic Acid Hydrogenation

Jiahua Zhou,[a] Yujun Zhao,[a,*] Jian Zhang,[a] Yue Wang,[a] Oliver Y. Gutiérrez,[b] Shengnian Wang,[c] Zhengxiang Li,[d] Peng Jin,[d,*] Shengping Wang,[a] Xinbin Ma,[a] Johannes A. Lercher[b,e]

A novel PtSn/NHSS bimetallic catalyst with N-doped hollow silica sphere as support was synthesized for the gas-phase hydrogenation of acetic acid to ethanol. Its specific activity exhibited 30% higher than that of PtSn/SiO₂ due to the enhanced surface exposure of Pt active sites, induced by the strong interaction between Pt and N.

Highly dispersed noble metal nanoparticle (NP) catalysts are widely used in heterogeneous reactions because of their excellent catalytic performance.[1, 2] Numerous researchers are focused on improving the utilization efficiency of precious metals by maximizing their dispersion because a higher dispersion increases the exposure of surface sites, their intrinsic reactivity due to under-coordination, and quantum effects, which results in superior catalytic performance of the involved noble metal NPs.[3-7]

However, owing to their thermodynamic instability, nanoparticles easily aggregate when enough energy is available to overcome diffusion barriers, resulting in the deactivation of the heterogeneous catalyst.[8] The strong metal-support interactions (SMSI) could stabilize well-dispersed metal NPs and prohibit their aggregation during thermal pre-treatment and under harsh reaction conditions.[9]

As a model reaction for the conversion of organic acids to the corresponding alcohols, the hydrogenation of acetic acid (AcOH) to ethanol (EtOH) has attracted much attention. Supported bimetallic noble-based catalysts such as Pt-Sn, Pt-Fe, Ru-Fe, Pd-Re have been reported to be effective for AcOH hydrogenation.[10-13] Among these catalysts, Pt-Sn catalysts exhibited higher catalytic activity and selectivity for the hydrogenation of AcOH to EtOH. For this dual-sites catalysis system, the role of Pt site is considered to provide mobile and activated hydrogen atoms,[14] and the dissociative adsorption of AcOH to acyl mainly depends on SnOₓ species which could provide Lewis acid sites. The reaction rate of AcOH hydrogenation could be determined by the formation of acyl species or reaction between H atoms and acyl species, depending on the ratio of the amount of Lewis acid sites to the amount of exposed Pt active sites.[15] Recently, we have developed a modified two-step sol-gel method (MTSG, Sn/SiO₂ support was prepared first by sol-gel (SG) process and then the Pt NPs were loaded by strong electrostatic adsorption method (SEA)) for the preparation of PtSn/SiO₂ catalysts.[16] An excellent activity was achieved in AcOH hydrogenation. However, further improving the utilization efficiency of Pt is still a challenge for this catalyst.

Nitrogen has been reported as a dopant to stabilize Pt catalysts on carbon surface, which presented higher activity in the decomposition of formic acid.[17] The stabilization effect of N on Pt catalyst led to the formation of electron-deficient, sub-nano Pt clusters with one order of magnitude higher activity than catalysts without N doping.[18] However, no research focused on the N doped PtSn/SiO₂ catalyst as well as the role of N on PtSn catalyst in acetic acid hydrogenation.

Herein, Sn supported on N-doped hollow silica spheres (Sn/NHSS) was facilely synthesized by a novel micelle and emulsion dual templating method (one-pot method).[19-22] The detailed preparation process of this one-pot method can be found in the ESI. A novel PtSn/NHSS catalyst with 0.5 wt.% Pt and 1 wt.% Sn was prepared and tested for the gas-phase hydrogenation of AcOH to EtOH, achieving excellent catalytic performance with 86.6% conversion of AcOH and 90.0% selectivity of EtOH under a WHSV of 1 h⁻¹ (Table S1). Compared with the PtSn/SiO₂ catalyst prepared by the MTSG method, and PtSn/N-SiO₂ post-treated by (3-Aminopropyl) triethoxysilane (APTES), the introduction of N using the one-pot method enhances the SMSI between Pt and N-doped Sn/HSS, and thus remarkably increasing the Pt dispersion. To the best of our

[a.] Key Laboratory for Green Chemical Technology of Ministry of Education. Collaborative Innovation Center of Chemical Science and Engineering, School of Chemical Engineering and Technology, Tianjin University, Tianjin 300072, China. Prof. Y. Zhao, E-mail: yujunzhao@tju.edu.cn

[b.] Institute for Integrated Catalysis, Pacific Northwest National Laboratory, Richland, WA99352, US.

[c.] Institute for Micromanufacturing, Louisiana Tech University, Ruston, LA71272, US.

[d.] School of Materials Science and Engineering, Hebei University of technology, Tianjin, 300130, China. Prof. P. Jin, E-mail: china.peng.jin@gmail.com

[e.] Department of Chemistry and Catalysis Research Center, TU München, Garching 85748, Germany.

knowledge, PtSn/NHSS catalyst is used for the first time in a gas-phase hydrogenation of AcOH to EtOH. The great improvement of this strategy on Pt specific activity gives a rational guideline on the preparation of industrial catalyst for hydrogenation of carboxylic acids.

The morphology and structure of the PtSn/NHSS catalyst was characterized by SEM and TEM. The SEM image (Fig. 1 (a)) shows that N-doped spherical silica nanoparticles with different particle sizes were successfully synthesized by the O/W microemulsions method. Numerous cracks on the surface of the silica spheres indicate high permeability of the silica shell, which provide mesoscale pathways for reactants/products, similar to what was reported by Yamashita et al.[22] Fig. 1 (b) shows that 0.5Pt1Sn/NHSS has a hollow silica structure with a shell thickness of approximately 18 nm. Besides, STEM and energy dispersive spectroscopy (EDS) mapping images further reveal the spatial distribution of Pt, Sn and N. As shown in Fig. 1 (c), Pt and Sn are dispersed evenly on the hollow silica sphere, indicating that Pt could be well anchored on the Sn/NHSS support.[18] Additionally, N is detected to be well dispersed on PtSn/NHSS (Fig. 1 (c)) and PtSn/N-SiO$_2$ catalysts (Fig. S4). The well dispersed N is believed to play an important role in the surface character of Pt catalysts. Based on the above analysis, a structural model for 0.5Pt1Sn/NHSS was proposed as shown in Fig. 1 (d), where Pt cluster and SnO$_x$ species are dispersed evenly on the hollow silica sphere, which might ensure the close contact between the Pt clusters and SnOx species, thus enhancing the synergy between Pt and Lewis acid sites. TEM images of the reduced catalysts are displayed in Fig. 2 and the particles of Pt in the samples are measured and listed in Table 1. The 0.5Pt1Sn/NHSS catalyst shows the smallest particle size of Pt (1.6 nm) and largest Pt dispersion (70%), while the Pt dispersion of 0.5Pt1Sn/SiO$_2$ and 0.5Pt1Sn/N-SiO$_2$ are only 50% and 46%, respectively. The results suggest that the post-treatment by N precursor could not promote Pt dispersed well. Conversely, Sn/NHSS support synthesized by the one-pot method could enhance the interaction between Pt and support, resulting in the higher dispersion of Pt. These observations confirm that the presence of N as electron and structure dopant helps anchoring Pt clusters and improving their dispersion.[18]

CO is preferentially adsorbed on Pt instead of Sn.[17, 23, 24] It has been reported that the irreversible adsorption of CO is weakened and even can become undetectable due to the ionic/electron-deficient state of Pt induced by N dopant.[4, 25, 26] This provides a direct method to characterize the effect of N on Pt. As listed in Table 1, the N-doped catalysts (0.5Pt1Sn/N-SiO$_2$ and 0.5Pt1Sn/NHSS) show similar CO/Metal$_{exposed}$ ratio of about 2900 µmol g$_{Pt}^{-1}$, which is
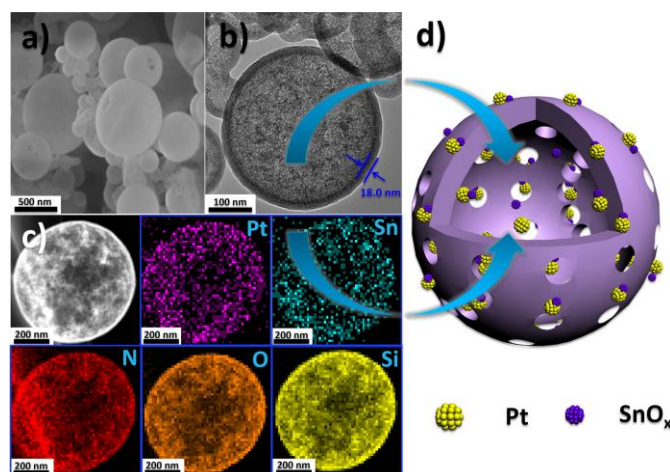

Fig. 1 (a) SEM, (b) TEM, (c) STEM image and the corresponding EDS mapping images of 0.5Pt1Sn/NHSS catalyst, (d) Schematic depiction of 0.5Pt1Sn/NHSS.

much lower than that of 0.5Pt1Sn/SiO$_2$ (5236 µmol g$_{Pt}^{-1}$). It suggests that CO adsorption on Pt is inhibited as the result of the modification effect by N, indicating the presence of strong interaction between Pt and the N-modified support. The low CO/Metal$_{exposed}$ ratio could result from the weakened backdonation of Pt d-electrons to π* antibonding orbital of CO due to the strong
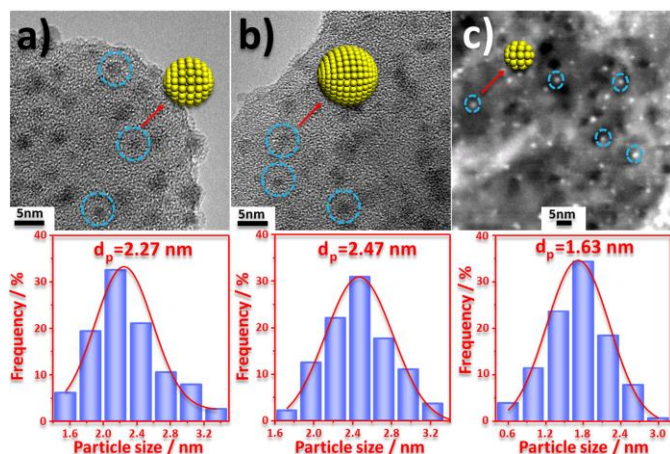

Fig. 2 TEM images of (a) 0.5Pt1Sn/SiO$_2$, (b) 0.5Pt1Sn/N-SiO$_2$; HAADF-STEM micrograph of (c) 0.5Pt1Sn/NHSS after reduction at 300 ˚C by H$_2$. Below are the particle size distributions of the Pt nanoparticles.

Table 1 Textural and physicochemical characteristics of catalysts.

Catalysts	Loading [a]			Content [b]	S$_{BET}$	D$_{pore}$	V$_{pore}$	D [c]	Pt dispersion [d]	CO/Metal$_{exposed}$ [e]
	Pt	Sn	N		(m^2 g^{-1})	(nm)	(cm^3·g^{-1})	(nm)	(%)	(µmol g$_{Pt}^{-1}$)
0.5Pt1Sn/SiO$_2$	0.47	1.27	-		407	3.8	0.33	2.27	50	5236
0.5Pt1Sn/N-SiO$_2$	0.59	1.21	3.0		404	3.7	0.24	2.47	46	2986
0.5Pt1Sn/NHSS	0.48	1.33	3.0		322	8.1	0.67	1.63	70	2839

[a] Determined by ICP-OES. [b] Nominal content. [c] Particle size determined by TEM. [d] Determined by TEM. [e] Determined by CO-chemisorption.

COMMUNICATION

interactions between Pt and N.[17] It is reasonable that the electronic state of the metal atoms was drastically changed because of the strong interaction with the N-doped support.

Density functional theory (DFT) calculations were then carried out to verify the electronic effects of N doping on Pt and compare the interactions between Pt and different supports. Based on the stable adsorption configurations for both Pt/SiO$_2$ and Pt/NHSS (Fig. S6), the plotted total density of state (TDOS) and partial density of state (PDOS) (Fig. S7) showed that the N atoms and Pt atoms both contributed to the density of state at the energy of 0 eV, indicating substantial Pt-N orbital overlaps around the Fermi level.[27] Consistent with the DOS analysis, NHSS exhibited larger adsorption energies (E$_{ads}$=-3.22 eV) in adsorbing Pt$_4$ cluster than SiO$_2$(E$_{ads}$=-1.26 eV), and the bond lengths of Pt-N (d$_{avg}$=2.03 Å) was shorter than Pt-O (d$_{avg}$=2.56 Å) (Table S2). These results revealed that Pt clusters on the reduced catalyst can be adsorbed much stronger by NHSS via N sites than by SiO$_2$ via O sites. When further considering the higher Pt dispersion of 0.5Pt1Sn/NHSS than 0.5Pt1Sn/N-SiO$_2$, it can be deduced that the current one-pot method for the preparation of the N-doped PtSn catalyst might prompt the homogeneous distribution of N species on the support, ensuring the intimate contact between Pt and N species during the reduction process. Thus, the contribution of N species on Pt dispersion is enhanced due to their strong interaction. The charge density difference was further calculated to verify the electronic effects of N doping on Pt (Fig. S8). It was found that more electron-deficient Pt species are formed in Pt/NHSS due to the electronic donation from Pt to N induced by the strong interaction between them. The difficulty in the reduction of the PtSn/NHSS catalyst can also well approve the suggested stronger interaction (Fig. S9).

Pt was loaded by strong electrostatic adsorption (SEA) method[28, 29] in this work. During the loading process, the silica surface was negatively charged by controlling the pH value of the impregnation solution to deprotonate the hydroxyl groups at the silica surface. Thus, the metal ammine complexes [Pt(NH$_3$)$_4$]$^{2+}$ could be easily absorbed onto the amorphous silica. Since the given pH value (10.60) was much higher than the PZC values[29] of the three supports (Fig. S10), the ability of these supports in adsorbing [Pt(NH$_3$)$_4$]$^{2+}$ should be identical according to the nature of the SEA method. Based on above results and discussions, hypothetical structural models of these catalysts were proposed as shown in Fig. 3. For 0.5Pt1Sn/N-SiO$_2$ catalyst, the post-treatment by N precursor (APTES) might result in the formation of -NH$_2$ on the support surface,[30] making Sn/SiO$_2$ positively charged. However, the small amount of APTES was used during the catalysts preparation, so that the PZC values can be hardly affected, which led to little influence on electrostatic adsorption of [Pt(NH$_3$)$_4$]$^{2+}$ on the Sn/N-SiO$_2$ support. Thus, the reduced 0.5Pt1Sn/N-SiO$_2$ presented a similar Pt dispersion with 0.5Pt1Sn/SiO$_2$ catalyst as the result of the nature of the post-treatment method. On the contrary, for Sn/NHSS support synthesized by one-pot method, N species are highly dispersed in the SiO$_2$ framework. The strong interaction between Pt and the support caused by N could help anchoring Pt species, increasing Pt dispersion on the NHSS support.

The catalytic performance of these catalysts was examined in AcOH hydrogenation under a WHSV of 2 h^{-1} (Fig. 4 (a)). Compared
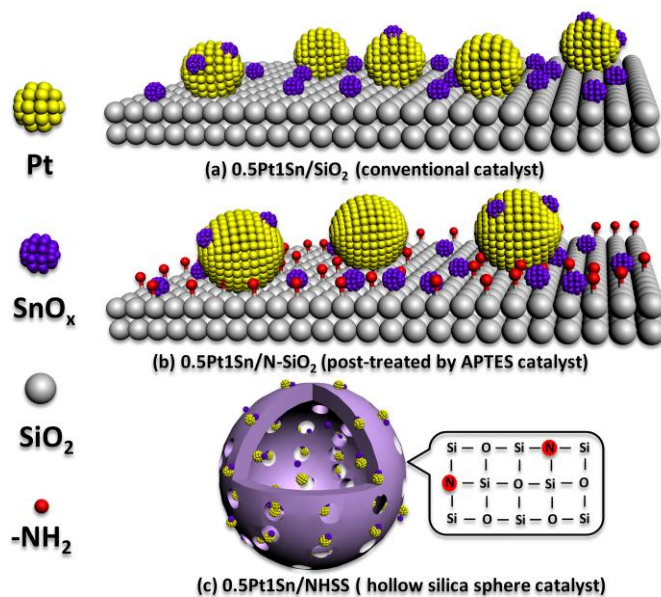

Fig. 3 Schematic structural representation of (a) 0.5Pt1Sn/SiO$_2$, (b) 0.5Pt1Sn/N-SiO$_2$, (c) 0.5Pt1Sn/NHSS catalysts.

with 0.5Pt1Sn/SiO$_2$ and 0.5Pt1Sn/N-SiO$_2$, 0.5Pt1Sn/NHSS exhibits the highest conversion of AcOH (67.1%) and EtOH selectivity (90.7%). In addition, the apparent activation barriers of the three catalysts are almost the same (51 kJ/mol, Fig. 4 (b)), indicating the N dopant does not affect the intrinsic catalytic activity of Pt. Thus, the large amount of exposed Pt sites for 0.5Pt1Sn/NHSS catalyst could provide affluent activated H atoms, which accelerates the reaction
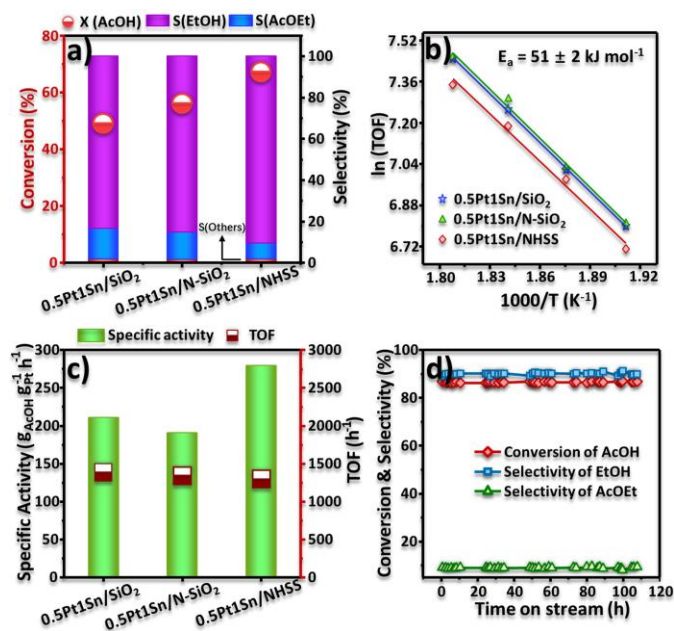

Fig. 4 (a) Catalytic performance. Reaction conditions: P=2.6 MPa, T=270 ˚C, H$_2$/AcOH=20, WHSV=2 h^{-1}; (b) TOF plot for the AcOH hydrogenation over the catalysts, R^2>0.99. (c) Specific activity and TOF of the catalysts. Reaction conditions: P=2.6 MPa, T=270 ˚C, H$_2$/AcOH=20, WHSV=2 h^{-1}. (d) Stability of 0.5Pt1Sn/NHSS, Reaction conditions: P=2.6 MPa, T=270 ˚C, H$_2$/AcOH=20, WHSV=1 h^{-1}.

rate between H and acyl species, promoting the conversion of AcOH and favouring the formation of EtOH. As reported by our previous work, the TOF of Pt sites on $PtSn/SiO_2$ remains nearly constant for the AcOH hydrogenation when the ratio of L/Pt (Lewis acid site/surface Pt site) is higher than 0.9.[16] In this work, the ratios of L/Pt of all the catalysts were higher than 1 (Table S3), which ensured an excess of Lewis acid sites. Thus, the dissociative adsorption of H_2 on Pt is the rate determination step and the increasing of the exposed Pt sites can effectively accelerate the hydrogenation rate. Different with the single active site mechanism,[31] above results should be ascribed to the nature of dual active sites mechanism. Therefore, the excellent performance of 0.5Pt1Sn/NHSS should be attributed to its highly exposed surface Pt sites, which is promoted by the enhanced metal-support interactions by N doping. Accordingly, the TOF calculated based on Pt sites remains nearly constant for the hydrogenation of AcOH (Fig. 4 (c)). Therefore, the apparent activity of the catalyst is only dependent on the amount of exposed Pt active sites instead of its ability in H_2 dissociation, which is also in accordance with the apparent activation barriers results (Fig. 4 (b)). Consequently, 0.5Pt1Sn/NHSS presents the highest specific activity of 279.67 g_{AcOH} g_{Pt}^{-1} h^{-1} due to the highest Pt dispersion among the three catalysts. The high Pt dispersion gives rise to more exposed Pt active sites to produce activated H atoms, resulting in excellent activity. It also exhibits excellent stability in AcOH hydrogenation (Fig. 4(d)), displaying a perspective future in heterogeneous catalysis.

In summary, a novel N-doped PtSn bimetallic nanocatalyst supported on hollow silica sphere was successfully synthesized. This was achieved by preparing the Sn/NHSS support first by one-pot (oil-in-water (O/W) microemulsions) method and sequentially Pt was loaded on Sn/NHSS by the SEA method. This is also the first time for the NHSS material to be applied as the support of PtSn catalyst and applied in the hydrogenation of organic acid. Compared with $0.5Pt1Sn/SiO_2$ and $0.5Pt1Sn/N-SiO_2$, 0.5Pt1Sn/NHSS exhibits much higher Pt dispersion because of the strong interaction between N and Pt as well as the highly dispersed N species in Sn/NHSS. Moreover, it showed an excellent specific activity in the hydrogenation of AcOH to EtOH. The NHSS material could be considered as an efficient support to anchor noble metals, giving an inspiration in the rational design of noble metal nanocatalysts for heterogeneous catalysis.

Conflicts of interest

There are no conflicts to declare.

Notes and references

[1] X. Li, M and Antonietti, *Chem Soc Rev*, 2013, **42**, 6593-6604.

[2] A. Dhakshinamoorthy and H. Garcia, *Chem Soc Rev*, 2012, **41**, 5262-5284.

[3] L. Li, A. Larsen, N. Romero, V. Morozov, C. Glinsvad, F. Abild-Pedersen, J. Greeley, K. Jacobsen and J. Norskov, *J Phys Chem Lett*, 2013, **4**, 222-226.

[4] G. Vile, D. Albani, M. Nachtegaal, Z. Chen, D. Dontsova, M. Antonietti, N. Lopez and J. Perez-Ramirez, *Angew Chem Int Ed Engl*, 2015, **54**, 11265-11269.

[5] J. Lin, B. Qiao, N. Li, L. Li, X. Sun, J. Liu, X. Wang and T. Zhang, *Chem Commun*, 2015, **51**, 7911-7914.

[6] H. Yan, H. Cheng, H. Yi, Y. Lin, T. Yao, C. Wang, J. Li, S. Wei and J. Lu, *J Am Chem Soc*, 2015, **137**, 10484-10487.

[7] B. Qiao, A. Wang, X. Yang, L. Allard, Z. Jiang, Y. Cui, J. Liu, J. Li and T. Zhang, *Nat Chem*, 2011, **3**, 634-641.

[8] X. Du, C. Zhao, Y. Luan, C. Zhang, M. Jaroniec, H. Huang, X. Zhang and S. Qiao, *J. Mater. Chem. A*, 2017, **5**, 21560-21569.

[9] J. Liu, *ChemCatChem*, 2011, **3**, 934-948.

[10] W. Rachmady and M. Vannice, *J. Catal.*, 2002, **209**, 87-98.

[11] V. Pallassana and M. Neurock, *J. Catal.*, 2002, **209**, 289-305.

[12] W. Li, L. Ye, J. Chen, X. Duan, H. Lin and Y. Yuan, *Catal. Today*, 2015, **251**, 53-59.

[13] S. Zhang, X. Duan, L. Ye, H. Lin, Z. Xie and Y. Yuan, *Catal. Today*, 2013, **215**, 260-266.

[14] G. Xu, J. Zhang, S. Wang, Y. Zhao and X. Ma, *Front. Chem. Sci. Eng.*, 2016, **10**, 417-424.

[15] W. Rachmady and M. Vannice, *J. Catal.*, 2002, **208**, 158-169.

[16] G. Xu, J. Zhang, S. Wang, Y. Zhao and X. Ma, *RSC Adv.*, 2016, **6**, 51005-51013.

[17] D. Bulushev, M. Zacharska, A. Lisitsyn, O. Podyacheva, F. Hage, Q. Ramasse, U. Bangert and L. Bulusheva, *ACS Catal.*, 2016, **6**, 3442-3451.

[18] L. Jia, D. Bulushev, O. Podyacheva, A. Boronin, L. Kibis, E. Gerasimov, S. Beloshapkin, I. Seryak, Z. Ismagilov and J. Ross, *J. Catal.*, 2013, **307**, 94-102.

[19] L. Han, C. Gao, X. Wu, Q. Chen, P. Shu, Z. Ding and S. Che, *Solid State Sci.*, 2011, **13**, 721-728.

[20] Y. Kuwahara, T. Yamanishi, T. Kamegawa, K. Mori and H. Yamashita, *ChemCatChem*, 2013, **5**, 2527-2536.

[21] Y. Kuwahara, T. Yamanishi, T. Kamegawa, K. Mori, M. Che and H. Yamashita, *Chem. Commun.*, 2012, **48**, 2882-2884.

[22] Y. Kuwahara, Y. Sumida, K. Fujiwara and H. Yamashita, *ChemCatChem*, 2016, **8**, 2781-2788.

[23] W. Michalak, J. Krier, S. Alayoglu, J. Shin, K. An, K. Komvopoulos, Z. Liu and G. Somorjai, *J. Catal.*, 2014, **312**, 17-25.

[24] M. Liu, W. Tang, Z. Xie, H. Yu, H. Yin, Y. Xu, S. Zhao and S. Zhou, *ACS Catal.*, 2017, **7**, 1583-1591.

[25] R. Arrigo, M. Schuster, Z. Xie, Y. Yi, G. Wowsnick, L. Sun, K. Hermann, M. Friedrich, P. Kast, M. Hävecker, A. Knop-Gericke and R. Schlögl, *ACS Catal.*, 2015, **5**, 2740-2753.

[26] E. Peterson, A. DeLaRiva, S. Lin, R. Johnson, H. Guo, J. Miller, J. Hun Kwak, C. Peden, B. Kiefer, L. Allard, F. Ribeiro, A. Datye, *Nat Commun*, 2014, **5**, 4885.

[27] L. Yao, W. Cao, M. Cao, *Curr. Appl Phys.*, 2016, **16**, 574-580.

[28] L. Jiao, J.R. Regalbuto, *J. Catal.*, 2008, **260**, 329-341.

[29] J.E. Samad, J. Blanchard, C. Sayag, C. Louis, J.R. Regalbuto, *J. Catal.*, 2016, **342**, 213-225.

[30] Y. Pei, C. Xiao, T. Goh, Q. Zhang, S. Goes, W. Sun, W. Huang, *Surf. Sci.,* 2016, **648**, 299-306.

[31] M. Huda and L. Kleinman, *Phys Rev B*, 2006, **74**, 195407 (1-7).